Induced-transparency in silicon-on-insulator based novel resonator systems

Danfeng Cui[1], Liping Wei[1], Chao Liu[2], Yaoying Liu[2], Yonghua Wang[2], Jun Liu[1,2], Chenyang Xue[1]

[1]*Ministry of Education, Key Laboratory of Instrumentation Science & Dynamic Measurement, North University of China, Taiyuan 030051, People's Republic of China*
[2]*Science and Technology on Electronic Test & Measurement Laboratory, Taiyuan 030051, People's Republic of China*
E-mail: xuechenyang@nuc.edu.cn

Published in Micro & Nano Letters; Received on 26th April 2013; Revised on 5th June 2013; Accepted on 12th June 2013

The coupled-resonator-induced-transparency (CRIT) phenomenon in a novel optical resonator system is experimentally demonstrated. The system is composed of a four-ring resonator with a 20 μm diameter on silicon, whose spectrum has a narrow transparency peak with low group velocity. The CRIT effect is observed in the optical coupled-resonator because of classical destructive interference. In this reported work, a CRIT resonance with a quality factor of 7.2×10^4 is demonstrated with the same cavity size and the power coupling of the system is 60%, which agree well with the theoretical analysis. Then, through and drop transmission spectra of the resonator coincide well with each other. Simultaneously, the detuning resonant wavelength can be controlled by changing the temperature.

1. Introduction: Nowadays, fabricating small structures using MEMS technology to control light has been excitingly developed in optical physics, and resonators which are capable of inducing coupled-resonator-induced-transparency (CRIT) can be widely used in fields such as optical sensors, the feedback cavity of a laser, optical filters and so on because of its resonance property and on-chip compatibility with other planar integrated optic devices. The phenomenon of CRIT is similar to the classical atomic resonance: electromagnetically induced transparency (EIT) and it works by means of coherent interference between resonating modes which produces optical transparency inside the absorption window. In a coupled resonant cavity, mutually independent resonant states interact by weak coupling effect between different cavities, thus changing the characteristics of the whole resonant system and generating CRIT [1].

In practice, it is challenging to detune the optical cavity to control the resonant interaction between the two optical pathways. For instance, the cascade of two indirectly coupled resonators [2, 3] requires an ~8 nm perimeter difference between the two rings, which is challenging to control in current experimental conditions. Furthermore, other existing configurations based on other coupled resonators [4, 5] proposed two almost identical resonators with different coupling strength and cavity losses. Although the coupling strength can be controlled in a passive manner, active tuning is required for controlling cavity losses, which adds complexity in device design and fabrication [6, 7].

In this Letter, we theoretically propose that CRIT transmission can be generated in a new structure which consists of ring resonators sandwiched by two indirectly coupled waveguides. The uniqueness of the proposed geometry compared with other systems is in the use of a quartcoupler, instead of a conventionally used directional coupler, which can obtain high a Q factor and delay the time of light travelling. The optical delay increases significantly because of multiple passes in the cavity. In addition, this geometry does not need precise calculation of the difference between the resonators' perimeters, which can lead to simplicity of the design and fabrication of the structure.

2. Theoretical analysis: The novel resonator systems consists of four-ring resonators evanescently side coupled with a pair of signal waveguides. When light is coupled into all the ring resonators, the four rings form a Fabry-Pérot (FP)-like cavity [8] shown by the black dotted line in Fig. 1*a*. We repeated the CRIT effect with four rings by analogy with that of two rings. The ring supports a travelling wave of amplitude $A(t)$, which is normalised as $A(t)^2$, representing the total power flowing through the ring waveguide at time t. The ring may also be viewed as a lumped oscillator of energy amplitude $a(t)$, normalised $|a(t)|^2$ represents the total energy stored in the ring. The incident wave is S_i, the filtered or detected wave is S_d and the transmitted wave is S_t.

With the developed coupled-mode-theory [9], it can be shown that the add-drop response in wavelength domain parameters of a fourth-order microring filter can be obtained by solving the following equation

$$\frac{\mathrm{d}}{\mathrm{d}t}a_4 = \left(j\omega_4 - \frac{1}{\tau_d}\right)a_4 - j\mu_4 a_2 - j\mu_5 a_3 \tag{1a}$$

$$\frac{\mathrm{d}}{\mathrm{d}t}a_3 = j\omega_3 a_3 - j\mu_5 a_4 - j\mu_3 a_2 - j\mu_2 a_1 \tag{1b}$$

$$\frac{\mathrm{d}}{\mathrm{d}t}a_2 = j\omega_2 a_2 - j\mu_4 a_4 - j\mu_3 a_3 - j\mu_1 a_1 \tag{1c}$$

$$\frac{\mathrm{d}}{\mathrm{d}t}a_1 = \left(j\omega_1 - \frac{1}{\tau_e}\right)a_1 - j\mu_1 a_2 - j\mu_2 a_3 - j\mu s_i \tag{1d}$$

Each ring oscillates at its own characteristic frequency ω_i, which in the sequel will all be set to equal. μ_n is the coupling coefficient between the rings and μ is the coupling coefficient between the bus waveguides and the outer rings. The terms represent the resonator couplings

$$\mu_n^2 = \kappa_n^2 \frac{v_{gn} v_{gn+1}}{(2\pi R_n)(2\pi R_{n+1})} \tag{2a}$$

$$\mu^2 = \frac{\kappa^2 v_{g1}}{2\pi R_1} = \frac{2}{\tau_e} \tag{2b}$$

where v_{gn} is the group velocity of ring n, R_n is the radius and κ_n^2 represents the corresponding power coupling coefficient. It has been assumed that the resonator's intrinsic losses are negligible.

Next, we consider the unidirectional propagation and partial coupling of light from a straight waveguide into four microring resonators coupled together. The absorption of the whole structure with only one ring reaches the maximum at resonance (ϕ is a multiple of 2π). When other rings are added to the structure, the absorption peak splits into two peaks and the absorption reaches the minimum at resonance [10]. Thus, a narrow transparent peak appears between the two split peaks, as shown in Fig. 2. As for

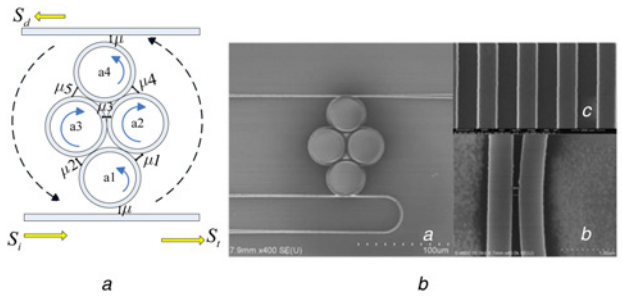

Figure 1 *Schematic drawing of fourth-order symmetrically coupled microring resonator (Fig. 1a); scanning-electron micrographs (Fig. 1b) of four-ring resonator (a), gap between bus waveguide and ring resonator (b), and grating (c)*

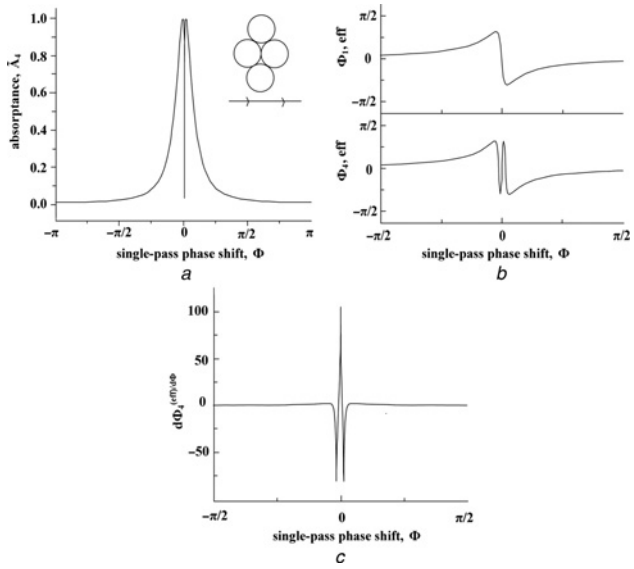

Figure 2 *Absorption against single-pass phase shift for four-coupled ring resonators with $a_1 = 0.9999$, $a_2 = 0.88$, $r_1 = 0.999$, $r_2 = 0.9$ (Fig. 2a); effective phase shift for single-ring resonator and for four-coupled ring resonators (Fig. 2b); slope of effective phase shift for four-coupled rings (Fig. 2c)*

the four-rings structure, its transmission coefficient is

$$\tau_4(\phi_4,\ \phi_3,\ \phi_2,\ \phi_1) = \frac{\gamma_4\sqrt{1-\gamma} - \alpha_4\tau_3(1-\gamma)e^{4i\phi}}{1-\gamma_4\alpha_4\tau_3\sqrt{1-\gamma}e^{4i\phi}} \quad (3)$$

where ω is the frequency of light. r_n , $t_n = \sqrt{1-\gamma^2}$, γ, α_n, $a_n = \exp(-\alpha L/2)$ and L_n are the reflection coefficient, permeability coefficient, insert loss, absorption coefficient, attenuation factor and length, respectively. The effective phase shift ϕ^{eff} of the whole structure is the argument of the transmission coefficient, which is

$$\phi^{\text{eff}}(\phi_4,\ \phi_3,\ \phi_2,\ \phi_1) = \arg(\tau_4) \quad (4)$$

From the above equation, we note that the transmission relies on the phase term ϕ, which can be described as

$$\phi(\omega) = \frac{\omega \text{Re}(n_{\text{eff}})L}{c} + \theta \quad (5)$$

where θ represents the reflective phase shifts, n_{eff} stands for the effective refractive index and c is light velocity in a vacuum.

Table 1 Propagation loss per round trip in microring resonators

W_{ring}, nm	400	450	500	550
Loss, dB/mm	31 ± 3	13 ± 1	7.5 ± 1	4.5 ± 0.5
$Q_{\text{intrinsic}}$	3000 ± 300	7000 ± 700	12 000 ± 1200	20 000 ± 2000

3. Fabrication and experiment: It is known that the microring with single mode whose width is < 600 nm at ~1.55 μm is ideal since other modes have higher propagation losses. With a reported method [11], propagation losses in fabricated microring resonators with radius ($R = 2.5$ μm) and different width (W_{ring}) were characterised and are listed in Table 1. The propagation loss decreases as the waveguide width increases in silicon waveguides, as the guided light is more confined in the silicon core and scatters less at the rough surfaces of the waveguides [12, 13]. Meanwhile, the radius in 20 μm can effectively inhibit bending loss. Hence, through comprehensive consideration of the theory and technology, we choose the waveguide width as 500 nm and the radius as 20 μm.

The top-view microscope image of the device fabricated on the silicon-on-insulator platform with a top silicon layer thickness of 220 nm and a buried oxide thickness of 3 μm is demonstrated in Fig. 1(*b*). It consists of a four-ring resonator with a diameter of 20 μm coupled with a pair of parallel silicon strip waveguides. The waveguides and the rings have widths of 500 and 600 nm, respectively, the distance between the straight waveguide and the rings is 120 nm, and the rings are tangent to each other.

The waveguides and rings were exposed in a 450 nm-thick positive resist (PMMA4) with the JBX-5500ZA 100 kV electron-beam Lithography system followed by inductively coupled plasma etching and the resulting structure is covered by a 2 μm-thick SiO_2 upper-cladding deposited by plasma-enhanced chemical vapour deposition, so that the silicon waveguides and rings are surrounded on all sides by oxide to reduce the propagation loss in microring resonators [14, 15].

The experimental setup for microcavity measurement is shown in Fig. 3. A tunable laser in the optical telecommunication band (NewFocus, 1550 nm wavelength band) was used to excite the microring resonant whispering gallery models linked to the strip waveguides. A polarisation controller is used to research the effect of different laser polarisation states to grating coupling efficiency. The input port of single-mode fibre connects to the polarisation controller and the output port constitutes the vertical coupling system with the Si waveguide grating to couple the light field into the straight waveguide. The transmission spectrum was collected by a photodetector and displayed on an oscilloscope. The coupling efficiency was greatly improved by using diffraction grating between the lensed fibres and the waveguide. Simultaneously, the input and output ports of fibres were placed on a high-precision three-axis adjustment stage to realise the angle between the single-mode fibre and the grating 10°. The approximate vertical coupling method can efficiently reduce the secondary reflection, so that it would improve light field coupling efficiency and mode matching. By

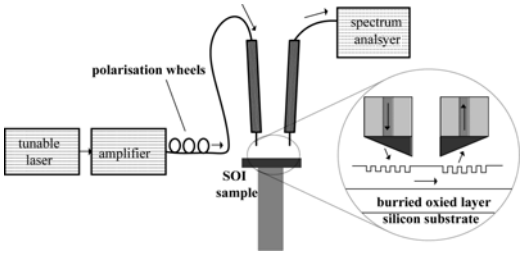

Figure 3 *Schematic of measurement platform*

doi: 10.1049/mnl.2013.0232

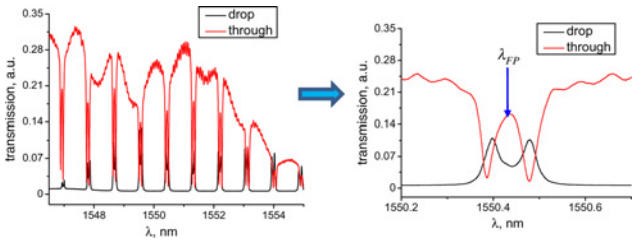

Figure 4 *Through and drop transmission spectra of resonator (red line shows through spectrum whereas black line shows drop)*

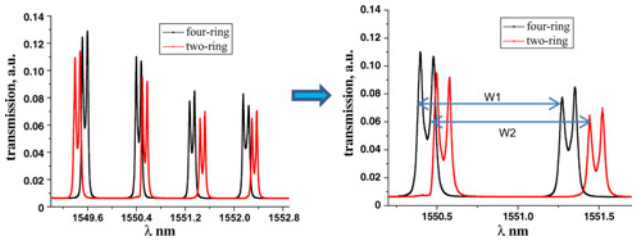

Figure 5 *Drop transmission spectra of two-ring and four-ring resonators*

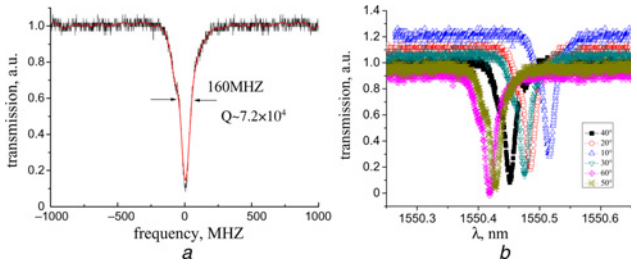

Figure 6 *Experimental responses of microring resonator (red line shows theoretical spectrum whereas black line shows measured) (Fig. 6a); thermal tuning of power transmission spectrum (Fig. 6b)*

using an infrared CCD camera and long focal distance CCD camera we could observe the chip and optical route clearly.

The structure presents a high-Q resonant mode when the low-Q resonances of all ring resonators couple coherently. Fig. 4 is the measured transmission spectrum which shows a narrow transmission peak inside a broader dip, similar to the transmission spectrum of an EIT system. When all ring resonators are out of resonance, light passes through the waveguide without coupling with the ring resonators, and the transmission is high. When light is coupled into one of the ring resonators, the resonator acts like a mirror reflecting the light from one waveguide into the other waveguide. The transmission thus shows a dip with full-width-half-maximum (FWHM) of 0.022 nm, corresponding to a quality factor of $Q = 72\,000$. The transmission spectrum of the device shows a peak at the resonant wavelength of the FP-like mode (λ_{FP}), which is in contrast to ordinary FP cavities because the fourth-ring resonator is still a travelling wave cavity with no back reflection into the input waveguide at any wavelength [2, 16, 17].

The drop transmission spectra of the two and the four-ring resonators are shown in Fig. 5. The transmission of the two rings shows a dip at FWHM of 0.077 nm, corresponding to a quality factor of $Q = 20\,000$, and the bandwidth of these is 0.945 nm ($W2$). Compared with the two rings, the quality factor of the four rings is higher and the bandwidth ($W1 = 0.873$ nm) is narrower.

The quality (Q) of a resonator is a measure of the structure's frequency selectivity. The Q is given by the time averaged stored energy per optical cycle, divided by the power coupled or scattered out of the resonator. Fig. 6*a* shows the transmission spectrum of the quasi-TE mode. The quality factor of the ring resonator was demonstrated to be as high as 7.2×10^4. That has a major effect on the field of silicon sensing applications. The resonant frequency is highly dependent on detuning between the four-ring resonators. To show variable frequency, we tune the resonance of each resonator thermally. Temperature increase induces an increase of the refractive index of silicon and a red-shift of the resonance of the ring resonators. By changing the temperature, the detuning resonant wavelength can be controlled, as shown in Fig. 6*b*.

4. Conclusion: We have experimentally demonstrated a CRIT resonance with a Q-factor of 72 000 using a four-ring resonator with the same diameters and power coupling of 60%. In contrast to previous reports, it presents a higher quality and it is interesting to note that similar transparency effect was also found in the novel resonator systems. Since the resonance features are significantly narrower in coupled resonators, the dispersion is much greater and the light is slower (or faster) than in single resonators. Simultaneously, the detuning resonant wavelength can be controlled by changing the temperature.

5. Acknowledgments: This work was supported by the National Natural Science Foundation (61076111). The authors thank the Suzhou Institute of Nano-Tech and Nano-Bionics of the Chinese Academy of Sciences for their kind assistance in the fabrication.

6 References

[1] Smith D.D., Chang H., Fuller K.A., Rosenberger A.T., Boyd R.W.: 'Coupled-resonator-induced transparency', *Phys. Rev. A*, 2004, **69**, article id 063804

[2] Xu Q., Sandhu S., Povinelli M.L., Shakya J., Fan S., Lipson M.: 'Experimental realization of an on-chip all-optical analogue to electromagnetically induced transparency', *Phys. Rev. Lett.*, 2006, **96**, (12), article id 123901

[3] Totsuka K., Kobayashi N., Tomita M.: 'Slow light in coupled-resonator-induced transparency', *Phys. Rev. Lett.*, 2007, **98**, (21), article id 213904

[4] Naweed A., Farca G., Shopova S.I., Rosenberger A.T.: 'Induced transparency and absorption in coupled whispering gallery microresonators', *Phys. Rev. A*, 2005, **71**, (4), article id 043804

[5] Heebner J.E., Boyd R.W.: '"Slow" and "fast" light in resonator-coupled waveguides', *J. Mod. Opt.*, 2002, **49**, pp. 2629–2636

[6] Almeida V.R., Barrios C.A., Panepucci R.R., Lipson M.: 'All-optical control of light on a silicon chip', *Nature*, 2004, **431**, pp. 1081–1084

[7] Chan S., Fauchet P.M.: 'Silicon microcavity light emitting devices', *Opt. Mater.*, 2001, **17**, pp. 31–34

[8] Han Z., Bozhevolnyi S.I.: 'Plasmon-induced transparency with detuned ultracompact Fabry-Perot resonators in integrated plasmonic devices', *Opt. Express*, 2011, **19**, (4), pp. 3251–3257

[9] Little B.E., Chu S.T., Haus H.A., Foresi J., Laine J.P.: 'Microring resonator channel dropping filters', *IEEE J. Lightwave Technol.*, 1997, **15**, pp. 998–1005

[10] Oishi T., Suzuki R., Sultana P., Tomita M.: 'Optical precursors in coupled-resonator-induced transparency', *Opt. Lett.*, 2012, **37**, (14), pp. 2964–2966

[11] Xiao S., Khan M.H., Shen H., Qi M.: 'Modeling and measurement of losses in silicon-on-insulator resonators and bends', *Opt. Express*, 2007, **15**, pp. 10553–10561

[12] Vlasov Y.A., McNab S.J.: 'Losses in single-mode silicon-on-insulator strip waveguides and bends', *Opt. Express*, 2004, **12**, pp. 1622–1631

[13] Lee H., Chen1 T., Li J., Painter O., Vahala K.J.: 'Ultra-low-loss optical delay line on a silicon chip', *Nature*, 2012, **3**, p. 867

[14] Lee K.K., Lim D.R., Kimerling L.C.: 'Fabrication of ultralow-loss Si/SiO_2 waveguides by roughness reduction', *Opt. Lett.*, 2001, **26**, pp. 1888–1890

[15] Dumon P., Bogaerts W., Wiaux V., *ET AL.*: 'Low-loss SOI photonic wires and ring resonators fabricated with deep UV lithography', *IEEE Photonics Technol. Lett.*, 2004, **16**, pp. 1328–1330

[16] Maleki L., Matsko A.B., Savchenkov A.A., Ilchenko V.S.: 'Tunable delay line with interacting whispering-gallery-mode resonators', *Opt. Lett.*, 2004, **29**, pp. 626–628

[17] Xu Q., Shakya J., Lipson M.: 'Direct measurement of tunable optical delays on chip analogue to electromagnetically induced transparency', *Opt. Express*, 2006, **14**, pp. 6463–6468

Micro & Nano Letters, 2013, Vol. 8, Iss. 10, pp. 619–622
doi: 10.1049/mnl.2013.0232